XLVI CILAMCE
VITÓRIA - ES - BRAZIL - 2025
XLVI IBERO-LATIN AMERICAN CONGRESS ON COMPUTATIONAL METHODS IN ENGENEERING

An extended Isogeometric Boundary Element formulation for the three-dimensional fatigue crack propagation modelling

Matheus Rocha[1], Jon Trevelyan[2], Edson D. Leonel[1]

[1]*Department of Structural Engineering, São Carlos School of Engineering, University of São Paulo*
Av. Trabalhador Sancarlense, 400, 13566-590, São Paulo, Brazil
rocha.matheus@usp.br, edleonel@sc.usp.br
[2]*Department of Engineering, Durham University*
South Road, DH1 3LE, Durham, United Kingdom
jon.trevelyan@durham.ac.uk

Abstract. The fatigue crack propagation is responsible for the failure of various engineering components, which justifies the importance of its proper modelling. Its accurate prediction in real-life applications requires a numerical approach to account for complex details in geometry, boundary conditions and mechanical response. In this sense, the Boundary Element Method (BEM) has proven to be a highly attractive approach to fracture mechanics applications, especially for three-dimensional models, since its boundary-only discretisation simplifies the re-meshing process and allows for the precise representation of the singular stress field near the crack front in these problems. The isogeometric approach in the BEM enables a smooth coupling with models built in CAD software. This stems from using the same approximation functions for the mechanical fields as these models use for their geometric description, in this study, the Non-Uniform Rational B-Splines (NURBS). However, the standard isogeometric BEM does not capture the asymptotic behaviour close to the crack front, and it also introduces a non-physical jump displacement at this region. The enrichment approach has been demonstrated to be a successful strategy to circumvent these issues, in which the Williams solution expands the displacement approximation close to the crack front. Additionally, it introduces Stress Intensity Factors (SIFs) parameters that directly interpolate them, dismissing the need for computationally costly strategies such as the J-integral. In this context, this study proposes the fatigue crack growth modelling with the eXtended Isogeometric Boundary Element Method (XIGABEM) in which the SIFs are directly obtained by the XIGABEM formulation. Two different crack growth criteria are responsible for the crack growth: the hoop stress and the Schollmann criteria. In addition, a curve fitting algorithm defines the new crack front by finding the position of both control points and weights. Furthermore, a fine-tuning strategy guarantees C^0 and C^1 continuity between adjacent patches, which is required by the enrichment functions and enables a multi-patch description of cracks. One numerical application demonstrates the robustness and accuracy of the proposed scheme through its comparison with a reference solution. Thus, the XIGABEM strategy demonstrates its suitability for the three-dimensional fatigue crack growth analysis.

Keywords: Boundary Element Method, Isogeometric Analysis, Fatigue analysis, Enrichment formulation, Crack growth.

1 Introduction

Fatigue crack propagation is a structural phenomenon in mechanical components subjected to cyclic loading. It is specially concerning because varying loading under operational conditions may lead to progressive crack growth due to intrinsic material flaws. Predicting the number of load cycles to failure is therefore essential to ensure structural safety and prevent catastrophic events during service. Understanding and modelling fatigue crack growth has consequently become a central topic in fracture mechanics and structural integrity assessment.

In this context, the Linear Elastic Fracture Mechanics (LEFM) provides the theoretical foundation for analysing crack behaviour under cyclic loads, with the Stress Intensity Factor (SIF) being a relevant parameter to characterise the crack driving force. However, analytical solutions for SIFs are only available for simple geometries, so that numerical methods become the most suitable approach for realistic three-dimensional analyses. The Finite Element Method (FEM) has been widely used for this purpose, but it suffers from high computational cost due to the need for refined meshes near the crack front and frequent re-meshing during crack propagation. Alternative

approaches, such as peridynamics, phase-field modelling, and the eXtended/Generalised FEM (X/GFEM), have been proposed to mitigate these drawbacks by improving the representation of discontinuities without extensive mesh modifications.

Boundary-based techniques present additional advantages for fatigue analysis. The Boundary Element Method (BEM) requires only boundary discretisation, inherently reducing the computational cost and simplifying crack growth simulations. Its combination with isogeometric analysis (IGA) leads to the Isogeometric BEM (IGABEM) [1], which directly exploits CAD boundary representations and improves the geometric accuracy of the model. Building on recent developments [2, 3], the eXtended IGABEM (XIGABEM) incorporates enrichment strategies that allow for direct determination of SIFs without complex post-processing. This paper presents a three-dimensional XIGABEM formulation for modeling fatigue crack propagation, incorporating a crack front update algorithm to define the new crack front position and comparing two propagation criteria applicable to mixed-mode conditions.

2 Extended Isogeometric Boundary Element Method for fracture mechanics

This section contains a brief description of the Extended Isogeometric Boundary Element Method (XIGABEM), which is based on established references for IGABEM [1] and its expansion for three-dimensional fracture mechanics [2, 3]. The Isogeometric Boundary Element Method arises from the application of the discretisation with NURBS over the solid boundary on the Somigliana Identity and its corresponding derivative. In addition, the Dual Boundary Element Method (DBEM) is responsible for enabling the boundary element formulation to account for the presence of cracks. This yields the discretised form of the boundary integral equations as:

$$\frac{\delta_{\ell k}}{2}\sum_{\alpha=1}^{n^\gamma}\phi_\alpha^{\hat{\gamma}}(\hat{\mathbf{x}}^{eb})d_k^\beta+\sum_{\gamma=1}^{NS}\underline{\mathrm{T}}_{\ell k}^{*\,\alpha\gamma}d_k^\beta=\sum_{\gamma=1}^{NS}\underline{\mathrm{U}}_{\ell k}^{*\,\alpha\gamma}p_k^\beta$$

$$\frac{\delta_{\ell k}}{2}\sum_{\alpha=1}^{n^\gamma}\phi_\alpha^{\hat{\gamma}+}(\hat{\mathbf{x}}^{c+})d_k^\beta+\frac{\delta_{\ell k}}{2}\sum_{\alpha=1}^{n^\gamma}\phi_\alpha^{\hat{\gamma}-}(\hat{\mathbf{x}}^{c-})d_k^\beta+\sum_{\gamma=1}^{NS}\underline{\mathrm{T}}_{\ell k}^{*\,\alpha\gamma}d_k^\beta=\sum_{\gamma=1}^{NS}\underline{\mathrm{U}}_{\ell k}^{*\,\alpha\gamma}p_k^\beta \tag{1}$$

$$\frac{1}{2}\sum_{\alpha=1}^{n^\gamma}\phi_\alpha^{\hat{\gamma}-}(\hat{\mathbf{x}}^{c-})p_j^\beta-\frac{1}{2}\sum_{\alpha=1}^{n^\gamma}\phi_\alpha^{\hat{\gamma}+}(\hat{\mathbf{x}}^{c+})p_j^\beta+n_\ell(\hat{\mathbf{x}}^{c-})\sum_{\gamma=1}^{NS}\underline{\mathrm{S}}_{k\ell j}^{*\,\alpha\gamma}d_k^\beta=n_\ell(\hat{\mathbf{x}})\sum_{\gamma=1}^{NS}\underline{\mathrm{D}}_{k\ell j}^{*\,\alpha\gamma}p_k^\beta,$$

in which $\delta_{\ell k}$ is the Kronecker delta, ϕ refers to the isogeometric basis function. $\hat{\mathbf{x}}$ denotes the location point and its superscripts eb, $c+$ and $c-$ indicate that it is positioned at the external boundary, in the upper or lower crack face, respectively. In addition, γ denotes a NURBS surface in the set that contains NS surfaces of the IGABEM discretization. The term n_ℓ denotes the normal outward vector. The coefficients d_k^β and p_k^β are parameters from which the displacement and traction distribution over the surface γ may be recovered using the following expressions:

$$\begin{aligned}u_k^\gamma(\xi_1,\xi_2)&=\phi_\alpha^\gamma(\xi_1,\xi_2)d_k^\beta\\ t_k^\gamma(\xi_1,\xi_2)&=\phi_\alpha^\gamma(\xi_1,\xi_2)p_k^\beta,\end{aligned} \tag{2}$$

in which the index β corresponds to a global connectivity between the local control point α on the surface γ for the approximation of the displacement ($u_k^\gamma(\xi_1,\xi_2)$) and the traction ($t_k^\gamma(\xi_1,\xi_2)$) fields for the parametric coordinates ξ_1 and ξ_2. The fundamental solution for the linear elasticity is part of $\underline{\mathrm{T}}_{\ell k}^{*\,\alpha\gamma}$, $\underline{\mathrm{U}}_{\ell k}^{*\,\alpha\gamma}$, $\underline{\mathrm{S}}_{k\ell j}^{*\,\alpha\gamma}$, and $\underline{\mathrm{D}}_{k\ell j}^{*\,\alpha\gamma}$, being:

$$\begin{aligned}\underline{\mathrm{T}}_{\ell k}^{*\,\alpha\gamma}&=\sum_{\mathrm{ks}=1}^{n_{\mathrm{ks}}^\gamma}\int_\Lambda T_{\ell k}^*\,\phi_\alpha^\gamma\,J_\gamma^{\mathrm{ks}}\,d\Lambda \qquad \underline{\mathrm{S}}_{k\ell j}^{*\,\alpha\gamma}=\sum_{\mathrm{ks}=1}^{n_{\mathrm{ks}}^\gamma}\int_\Lambda S_{k\ell j}^*\,\phi_\alpha^\gamma\,J_\gamma^{\mathrm{ks}}\,d\Lambda\\ \underline{\mathrm{U}}_{\ell k}^{*\,\alpha\gamma}&=\sum_{\mathrm{ks}=1}^{n_{\mathrm{ks}}^\gamma}\int_\Lambda U_{\ell k}^*\,\phi_\alpha^\gamma\,J_\gamma^{\mathrm{ks}}\,d\Lambda \qquad \underline{\mathrm{D}}_{k\ell j}^{*\,\alpha\gamma}=\sum_{\mathrm{ks}=1}^{n_{\mathrm{ks}}^\gamma}\int_\Lambda D_{k\ell j}^*\,\phi_\alpha^\gamma\,J_\gamma^{\mathrm{ks}}\,d\Lambda,\end{aligned} \tag{3}$$

in which the numerical integration takes place along the Gaussian space $\Lambda=[-1,1]\times[-1,1]$, $T_{\ell k}^*$, $U_{\ell k}^*$, $S_{k\ell j}^*$ and $D_{k\ell j}^*$ refers to the fundamental solutions for three-dimensional linear elasticity [1], and J_γ^{ks} is the resulting Jacobian from a transformation from the integration space to the physical space passing through the NURBS

parametric space. The application of eq. (1) into all collocation points whose position is defined by the Greville Abscissae strategy [1, 4] results in the algebraic system $\mathbf{Hd} = \mathbf{Gp}$. The boundary conditions incorporation over this system yields a final system $\mathbf{Ax} = \mathbf{b}$, in which $\mathbf{x}$ stores the unknowns in displacement and traction coefficients. Its solution results in the necessary parameters to obtain the mechanical fields along the boundary.

The expansion of the displacement approximation field with the inclusion of the first term of the Williams solution as the enrichment function results in the XIGABEM formulation for three-dimensional fracture mechanics as:

$$u_k^{\gamma^{+/-}}(\xi_1,\xi_2) = \sum_{\alpha=1}^{n^\gamma} \phi_\alpha^{\gamma^{+/-}}(\xi_1,\xi_2) d_k^\beta + \sum_{s=1}^{n_K^\gamma} \tilde{\phi}_s^{\mathrm{cf}}(t) R_{kq}^{\mathrm{cf}} \psi_{qM}^{\bar{\gamma}^{\mathrm{cf}}} \tilde{K}_M^{s\,\mathrm{cf}}, \tag{4}$$

in which $\tilde{\phi}_s^{\mathrm{cf}}(t)$ is the unidirectional NURBS basis function on the crack front cf taken as the same from the crack surface, and interpolates the SIF coefficients $\tilde{K}_M^{s\,\mathrm{cf}}$. Each crack front incorporates n_K^γ additional SIF interpolation parameters along the front. The enrichment function ψ_{qM} is:

$$\psi_{qM} = \begin{bmatrix} \psi_{nI} & \psi_{nII} & \psi_{nIII} \\ \psi_{bI} & \psi_{bII} & \psi_{bIII} \\ \psi_{tI} & \psi_{tII} & \psi_{tIII} \end{bmatrix} \quad \begin{aligned} \psi_{nI} &= \frac{1}{2\mu}\sqrt{\frac{r^t}{2\pi}}\cos\left(\frac{\theta^t}{2}\right)\left[\kappa - 1 + 2\sin^2\left(\frac{\theta^t}{2}\right)\right] \\ \psi_{nII} &= \frac{1}{2\mu}\sqrt{\frac{r^t}{2\pi}}\sin\left(\frac{\theta^t}{2}\right)\left[\kappa + 1 + 2\cos^2\left(\frac{\theta^t}{2}\right)\right] \\ \psi_{bI} &= \frac{1}{2\mu}\sqrt{\frac{r^t}{2\pi}}\sin\left(\frac{\theta^t}{2}\right)\left[\kappa + 1 - 2\cos^2\left(\frac{\theta^t}{2}\right)\right] \\ \psi_{bII} &= -\frac{1}{2\mu}\sqrt{\frac{r^t}{2\pi}}\cos\left(\frac{\theta^t}{2}\right)\left[\kappa - 1 - 2\sin^2\left(\frac{\theta^t}{2}\right)\right] \\ \psi_{tIII} &= \frac{1}{2\mu}\sqrt{\frac{r^t}{2\pi}}4\sin\left(\frac{\theta^t}{2}\right) \\ \psi_{tI} &= \psi_{tII} = \psi_{nIII} = \psi_{bIII} = 0, \end{aligned} \tag{5}$$

having r^t as geometrical properties related to the point $P(\xi_1,\xi_2)$ at the enriched surface, while κ is the Kolosov constant associated to the crack front stress state, being $\kappa = 3 - 4\nu$ for plane-strain and $\kappa = \frac{3-\nu}{1+\nu}$ for plane-stress. The XIGABEM approach combines this enrichment set of functions with the rotation matrix R_{kq}^{cf}, which yields $\tilde{K}_M^{s\,\mathrm{cf}}$ directly being SIF parameters. The rotation matrix comes from the Frenet-Serret approach, which is suitable for defining it based on parametric representation of curves. The impact of this enrichment on the algebraic system results in an additional set of unknowns without adding new equation. Then, a compatibility strategy ensures a tying between upper and lower crack surfaces at the crack front, which also introduces the amount of equations required for the system to remain square. The in-depth explanation of these concepts is present in Rocha, Trevelyan and Leonel [2]. After solving the algebraic system, the SIF parameters are directly obtained, which dismisses computationally costly techniques for their extraction, as the J-integral.

3 Fatigue crack propagation with XIGABEM

This section presents the concepts related to the crack propagation framework considering high-cycle fatigue scenario. In this case, it is possible to predict the crack evolution using linear elastic fracture mechanics concepts, in which the SIFs become the main parameter for this analysis. Then, this analysis becomes natural for the three-dimensional XIGABEM for fracture mechanics, since the SIFs are directly the outputs of the method.

3.1 Crack growth criteria

The crack growth criterion defines the new position of the crack front based on the SIF state at its current position by defining the propagation angle θ_p. It must be noticed that the maximum hoop stress criterion does not consider the Mode III in the crack propagation angle, which justifies the use of the Schollmann criterion [5] to incorporate its effects on the crack growth process.

The maximum hoop stress criterion computes the θ_p direction in which the hoop stress is maximised for a given loading scenario and the equivalent SIF K_{eq} that incorporates the mode III effects is [6]:

$$\theta_p = 2\arctan\left[\frac{-2(K_{II}/K_I)}{1+\sqrt{1+8(K_{II}/K_I)^2}}\right] \qquad K_{eq} = \sqrt{K_I^2 + K_{II}^2 + (1+\nu)K_{III}^2} \tag{6}$$

The K_{eq} contains the influence of mode III through K_{III}, whereas the crack propagation angle does not take this mode into account. Thus, mixed-mode fracture problems having a non-zero mode III component may not be properly represented by this criterion. On the other hand, the Schollmann criterion defines the propagation angle such that it maximises the principal stress $\sigma_1^{'}$ in the local coordinate system defined on the crack front. By assuming $\sigma_{\bar{x}3} = 0$, the equivalent SIF is:

$$\begin{aligned} K_{eq} = \frac{1}{2}\cos\left(\frac{\theta_p}{2}\right)\Bigg\{ & K_I\cos^2\left(\frac{\theta_p}{2}\right) - \frac{3}{2}K_{II}\left(\sin\theta_p\right) \\ & + \sqrt{\left[K_I\cos^2\left(\frac{\theta_p}{2}\right) - \frac{3}{2}K_{II}\left(\sin\theta_p\right)\right]^2 + 4K_{III}^2}\Bigg\} \end{aligned} \tag{7}$$

and the equation for the propagation angle θ_p, which requires a Golden Section algorithm for its solution, is:

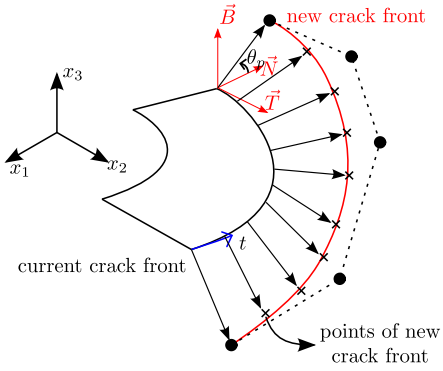
$$\begin{aligned} \Theta = \frac{1}{8\sqrt{2\pi r}}\Bigg\{ & \frac{-K_I\bar{S}}{2} - K_{II}\bar{C}_1 + \frac{1}{2}\Bigg[2\left[\left(K_I\bar{C}_2 - K_{II}\bar{S}\right) - K_{II}\bar{C}_1\right]\left[\frac{-K_I\bar{S}}{2} - K_{II}\bar{C}_1\right] \\ & -16K_{III}^2\sin\left(\theta_p\right)\Bigg]\left[\left[K_I\bar{C}_2 - K_{II}\bar{S}\right]^2 + 64K_{III}^2\cos^2\left(\frac{\theta_p}{2}\right)\right]^{-\frac{1}{2}}\Bigg\} = 0 \\ \bar{C}_1 = \frac{3}{2}\cos\left(\frac{\theta_p}{2}\right) + \frac{9}{2}\cos\left(\frac{3\theta_p}{2}\right) \\ \bar{C}_2 = 3\cos\left(\frac{\theta_p}{2}\right) + \cos\left(\frac{3\theta_p}{2}\right) \\ \bar{S} = 3\sin\left(\frac{\theta_p}{2}\right) + 3\sin\left(\frac{3\theta_p}{2}\right) \end{aligned} \tag{8}$$

3.2 Crack front update algorithm

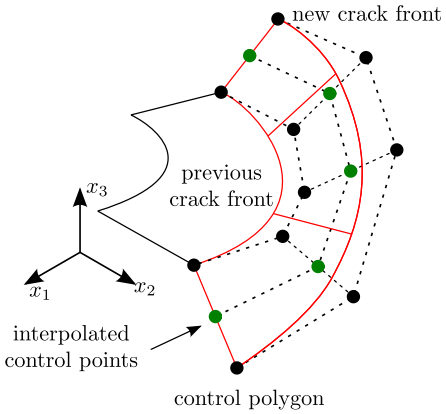
The crack front update algorithm defines the new crack front position by computing the crack front vector based on the propagation angle and the given crack front step Δa. Its definition occurs point-wise, and subsequently a NURBS curve whose knot vector is the same as the previous crack front, as shown in Fig. 1a. The determination of the position of the new control points and its corresponding weights relies on a curve fitting optimization of the NURBS curve for each new crack front point, as discussed in [3]. After the definition of the new crack front NURBS curve, the corresponding NURBS surface consists of an interpolation of the control points positions along the propagation direction, as illustrated in Fig. 1b. Further, the enrichment matrices are updated for the new crack front and the corresponding influences from the new surfaces over the standard IGABEM enlarges the algebraic system. This procedure occurs at each propagation step.

4 Numerical application

The numerical application of this study is the fatigue crack growth analysis of a penny-shaped crack with radius $R = 0.1$m inclined by $\pi/4$rad and located in the centre of a cube with side $a = 2.0$m, as shown in Fig. 2a. An amount of 10 NURBS surfaces describes each crack surface, being 5 bi-quadratic NURBS for each side, according to Fig. 2b. The final isogeometric mesh results from a knot-insertion approach over the initial geometry, and the total number of collocation points is 274. The upper face $x_2 = 1.0$ is subjected to a load varying cyclically between $\sigma_2^{\min} = 0$MPa and $\sigma_2^{\max} = 1$MPa. The loading condition results in a fully mixed mode I/II/III response due to the crack inclination. Pereira, Duarte and Xiao [7] analysed this geometry with the hp-generalised FEM approach, in which the Schollmann criterion defined the crack growth direction for the crack, and their results are taken as reference. The material and fatigue properties are: Young Modulus $E = 1000$MPa, Poisson's ratio $\nu = 0.3$, Paris constant $C = 1.5463.10^{-11}$, Paris exponent $m = 2.1$, and maximum increment $\Delta a_{\max} = 0.0185$m. The Paris constants assumed the units used for ΔK and da/dN to be MPa mm$^{0.5}$ and mm/cycle. The fatigue



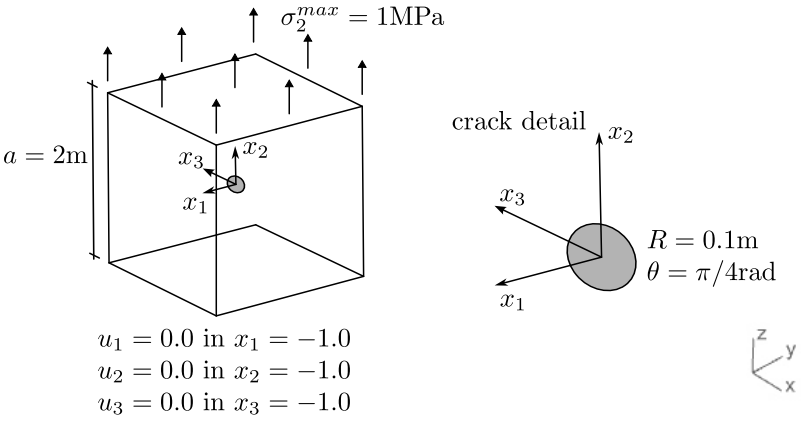
(a) Propagation of current crack front to define the new crack front points.



(b) Determination of NURBS surface control points from the new front.

Figure 1. Definition of new crack front and surface control points.

analysis considers 20 propagation steps. The hoop stress and the Schollmann criteria are applied, considering or not the K_{III} effect in the solution to compare against the corresponding solutions from the reference.



(a) Geometry and boundary conditions.

(b) Isogeometric mesh and control points.

Figure 2. Geometry, boundary conditions and isogeometric discretizetion of inclined penny-shaped crack under tensile fatigue loading.

The crack configurations for the initial geometry, and for the steps 7, 14 and 20 are presented in Fig. 3, considering both hoop stress and Schollmann criteria and the presence or absence of K_{III} in the propagation analysis. The crack grows from a fully mixed I/II/III response to a fully mode I SIF behaviour. In addition, the final geometry has a similar format as the reference solution, for all analysed scenarios. This suggests that the choice for the crack growth criteria does not significantly alter the final configuration in the XIGABEM formulation. This has not been observed in the reference solution, in which a significant difference between them was observed. In addition, the XIGABEM results align better with the expected K_{III} vanishing behaviour in comparison to the hp-GFEM approach. It is worth mentioning that the number of degrees of freedom in the last propagation step is 8082, which indicates that the XIGABEM formulation obtains accurate solution for this cracked problem with a small number of degrees of freedom. The comparison of the SIFs for all analysed scenarios, shown in Fig. 4, also demonstrates a good agreement in K_I between the XIGABEM results and the reference [7]. However, the K_{III} SIF does not vanish in the hp-GFEM analysis while it does in the XIGABEM results, which is associated with the final crack configuration of the XIGABEM. In summary, it is possible to attest that the XIGABEM results corroborate its suitability in the fatigue crack growth analysis of three-dimensional cracks.

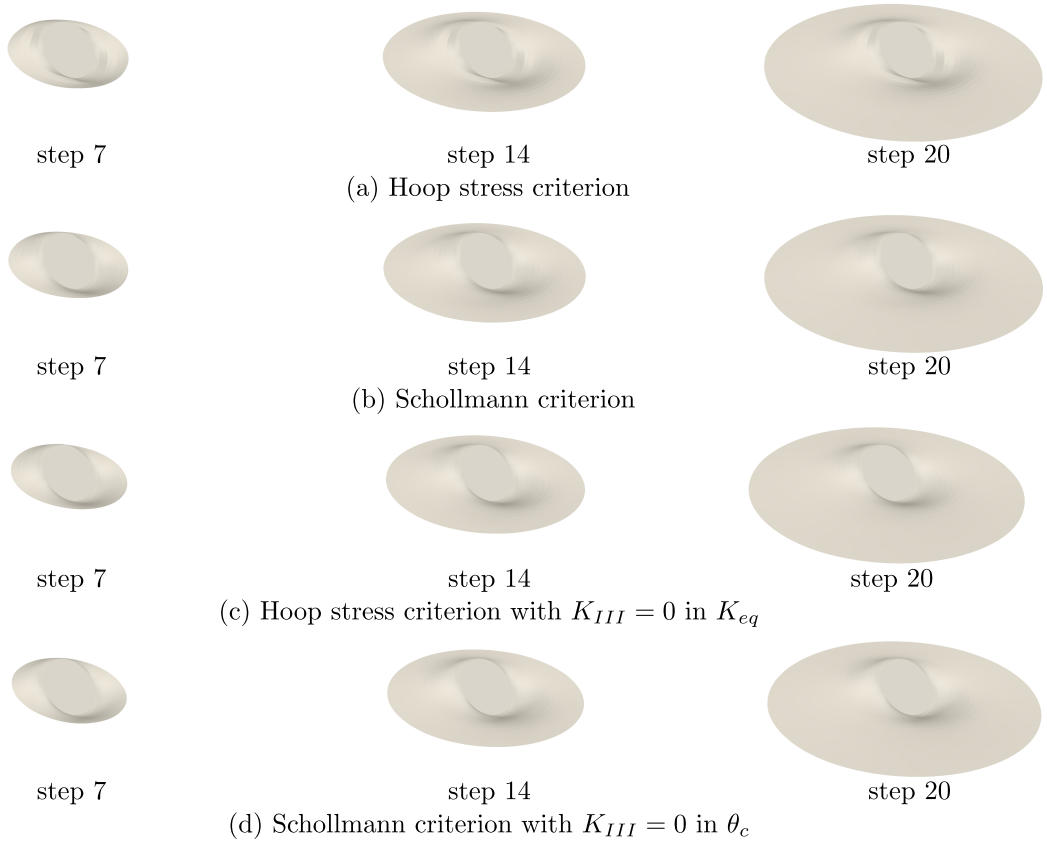


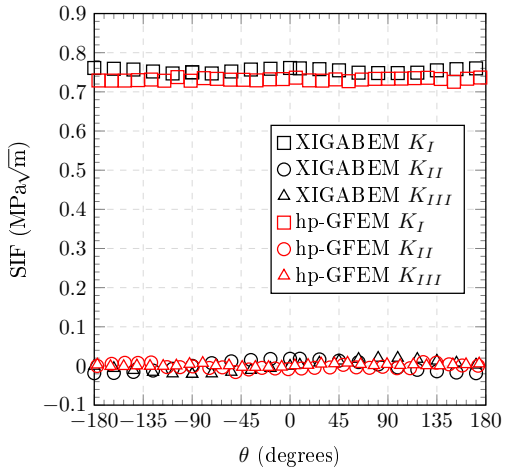
Figure 3. Inclined penny-shaped crack configuration during fatigue crack propagation with XIGABEM using (a) the Hoop stress criterion, (b) the Schollmann criterion, (c) the hoop stress criterion with $K_{III} = 0$, and (d) the Schollmann criterion with $K_{III} = 0$.

5 Final remarks

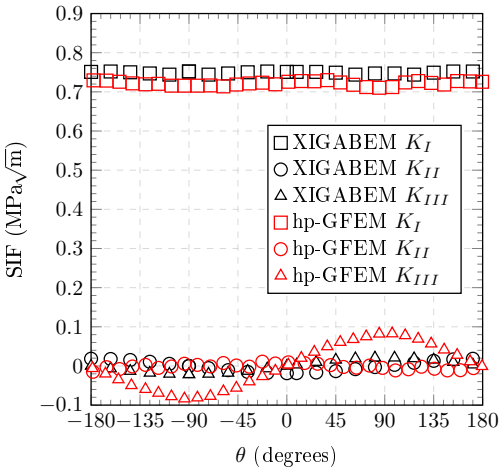
This study presented the fatigue crack propagation analysis with the eXtended Isogeometric Boundary Element Method (XIGABEM). The formulation relies solely on the boundary discretisation for the mechanical description of the solid under study. The isogeometric approach allows for a precise representation of curved surfaces and it reduces the geometrical error of the formulation. The enrichment functions are based on the Williams solution, and they directly incorporate the SIFs on the solution vector. These aspects result in a robust formulation for handling fracture mechanics, specifically high-cycle fatigue crack growth. One numerical application of a fully three-dimensional crack propagation analysis yields similar results to the reference, which demonstrates the accuracy of the developed formulation. Two crack growth criteria are compared, and the corresponding results are similar, which differs from the hp-GFEM approach. Thus, the formulation herein presented can be extended to other numerical analyses, as the low-cycle fatigue analysis and when the crack crosses the external boundary.

Acknowledgements. Sponsorship of this research project by the grants no 2019/18795-6 and 2022/00714-2 by the São Paulo Research Foundation (FAPESP) is greatly appreciated.

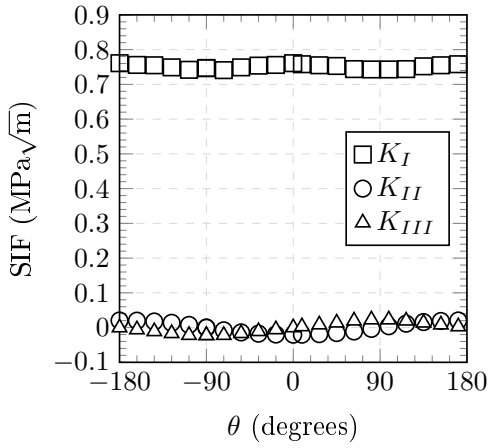
Authorship statement. The authors hereby confirm that they are the sole liable persons responsible for the authorship of this work, and that all material that has been herein included as part of the present paper is either the property (and authorship) of the authors, or has the permission of the owners to be included here.



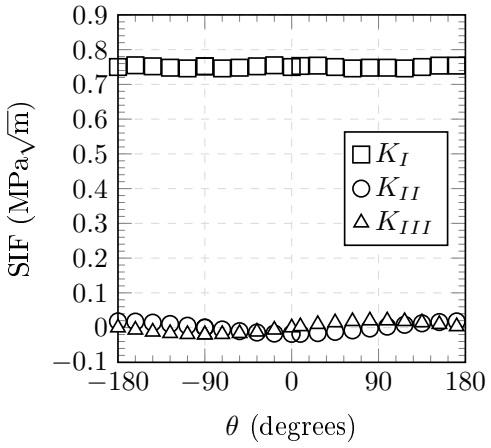
(a) $K_{III} \neq 0$ (Schöllmann criterion).



(b) $K_{III} = 0$ (Schöllmann criterion).



(c) $K_{III} \neq 0$ (Hoop stress criterion).



(d) $K_{III} = 0$ (Hoop stress criterion).

Figure 4. Comparison between hp-GFEM [7] and XIGABEM results for the SIFs at the final propagation step: (a)–(b) based on the Schöllmann criterion, and (c)–(d) using the hoop stress criterion, with and without the twist SIF K_{III}.

References

[1] G. Beer, B. Marussig, and C. Duenser. *The isogeometric boundary element method*. Springer, 2020.

[2] M. Rocha, J. Trevelyan, and E. D. Leonel. An extended isogeometric boundary element formulation for three-dimensional linear elastic fracture mechanics. *Computer Methods in Applied Mechanics and Engineering*, vol. 423, pp. 116872, 2024.

[3] M. Rocha, J. Trevelyan, and E. D. Leonel. Fatigue growth modelling of three-dimensional cracks with the extended isogeometric boundary element method. *Engineering Analysis with Boundary Elements*, vol. 177, pp. 106263, 2025.

[4] T. Greville. Numerical procedures for interpolation by spline functions. *Journal of the Society for Industrial and Applied Mathematics, Series B: Numerical Analysis*, vol. 1, n. 1, pp. 53–68, 1964.

[5] M. Schöllmann, H. A. Richard, G. Kullmer, and M. Fulland. A new criterion for the prediction of crack development in multiaxially loaded structures. *International Journal of Fracture*, vol. 117, pp. 129–141, 2002.

[6] W. H. Gerstle. *Finite and boundary element modelling of crack propagation in two and three dimensions using interactive computer graphics*. Phd thesis, Cornell University, New York, 1986.

[7] J. Pereira, C. A. Duarte, and X. Jiao. Three-dimensional crack growth with hp-generalized finite element and face offsetting methods. *Computational Mechanics*, vol. 46, pp. 431–453, 2010.